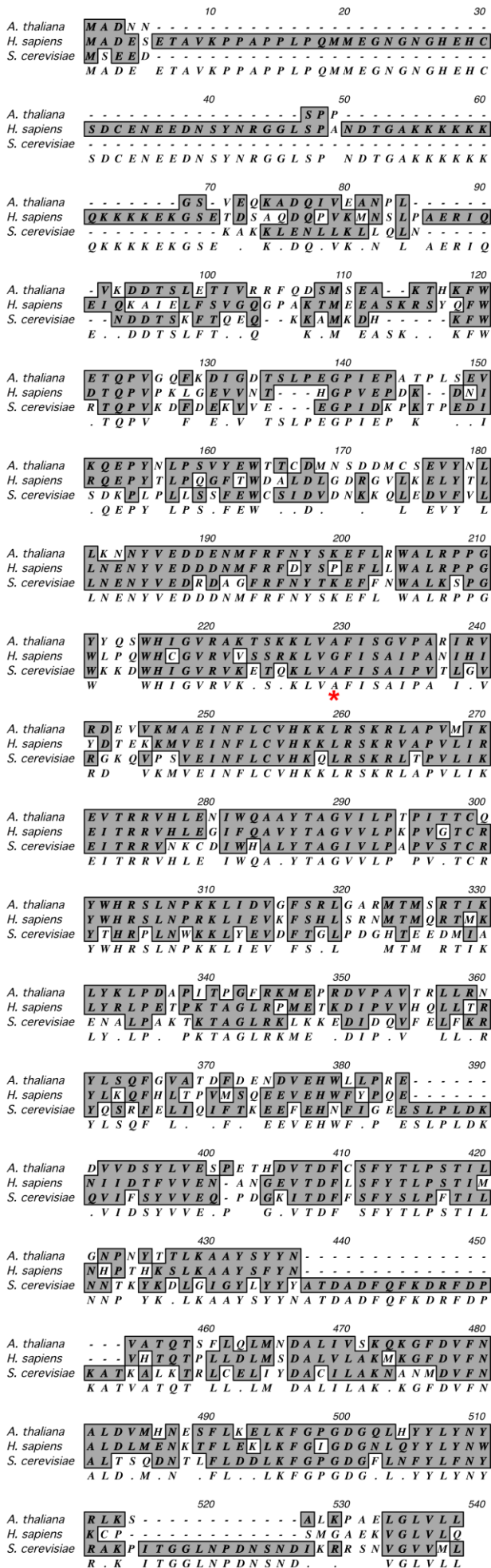




Supplemental Figure 1. Plant phenotype.

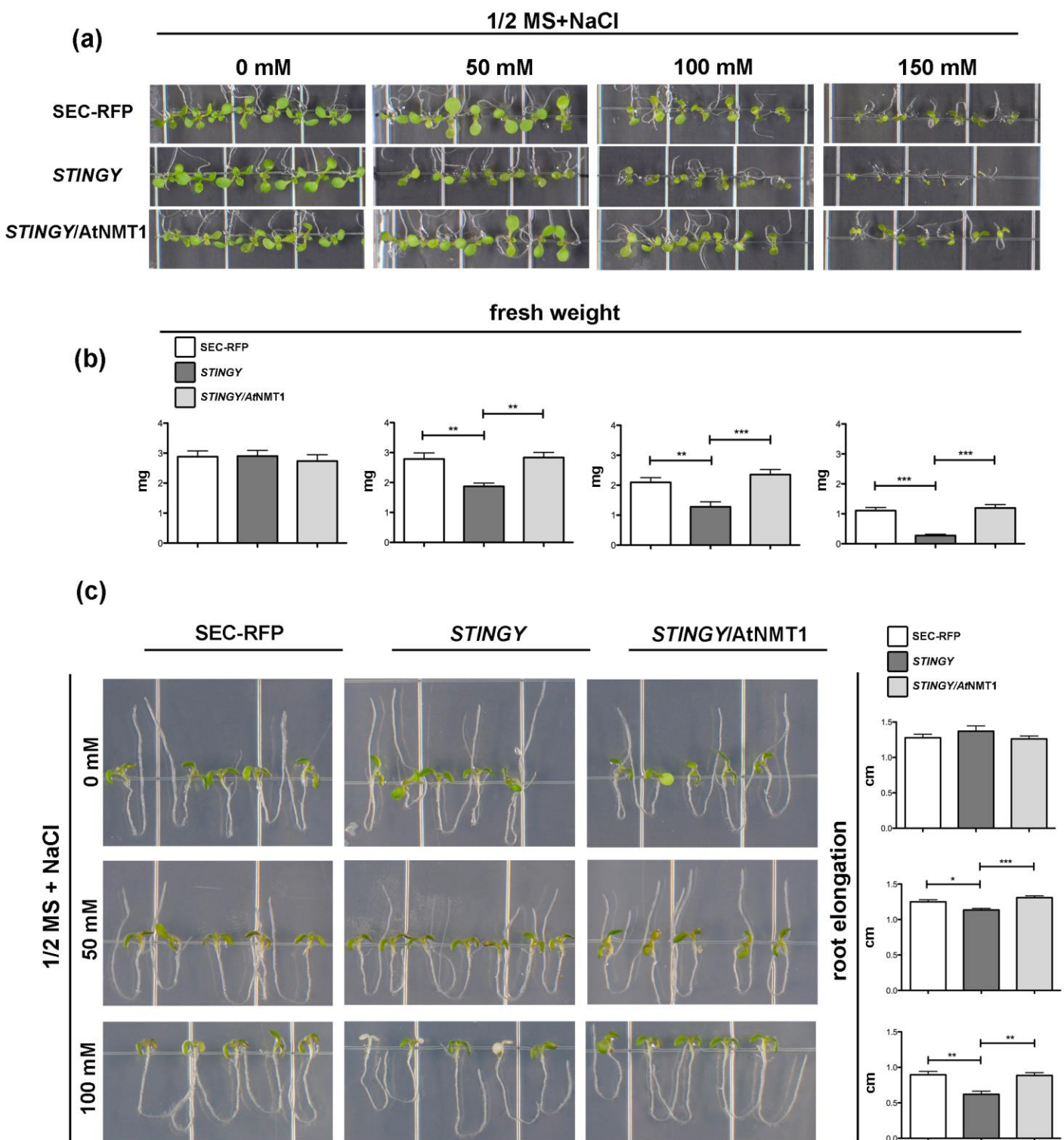
Comparison of plant phenotype of 4-week-old-plants with the following backgrounds: wild-type Col0, Col0/SEC-RFP, complemented *STINGY*/NMT1 and *STINGY* shows no obvious defects in the plant phenotype with the exception of a late flowering phenotype in *STINGY*.

Formatted Alignments



Supplemental Figure 2. Alignment of *A. thaliana*, *H. sapiens* and *S. cerevisiae* NMT1 sequences.

Protein sequence alignment run with ClustalW 2.1 highlights that the mutated amino acid A160 is in a conserved region in the catalytic region of the human NMT1. The alanine residue corresponds to a glycine residue in the human NMT1 (red asterisk in the alignment).



Supplemental Figure 3. Complementation of the *STINGY* salt sensitivity by *NMT1*.

a) Phenotype of Col0/SEC-RFP, *STINGY* and *STINGY/NMT1* grown on media either without NaCl or containing various NaCl concentrations.

b) Fresh weight of 10-day-old Col0/SEC-RFP, *STINGY* and *STINGY/NMT1* seedlings. Note that the fresh weight of *STINGY* is significantly affected ($p < 0.001$) as the salt concentration in the media increases compared to the other two backgrounds. The phenotype is rescued in homozygous seedlings expressing wild-type *NMT1*. Sample size ≥ 20 seedling each.

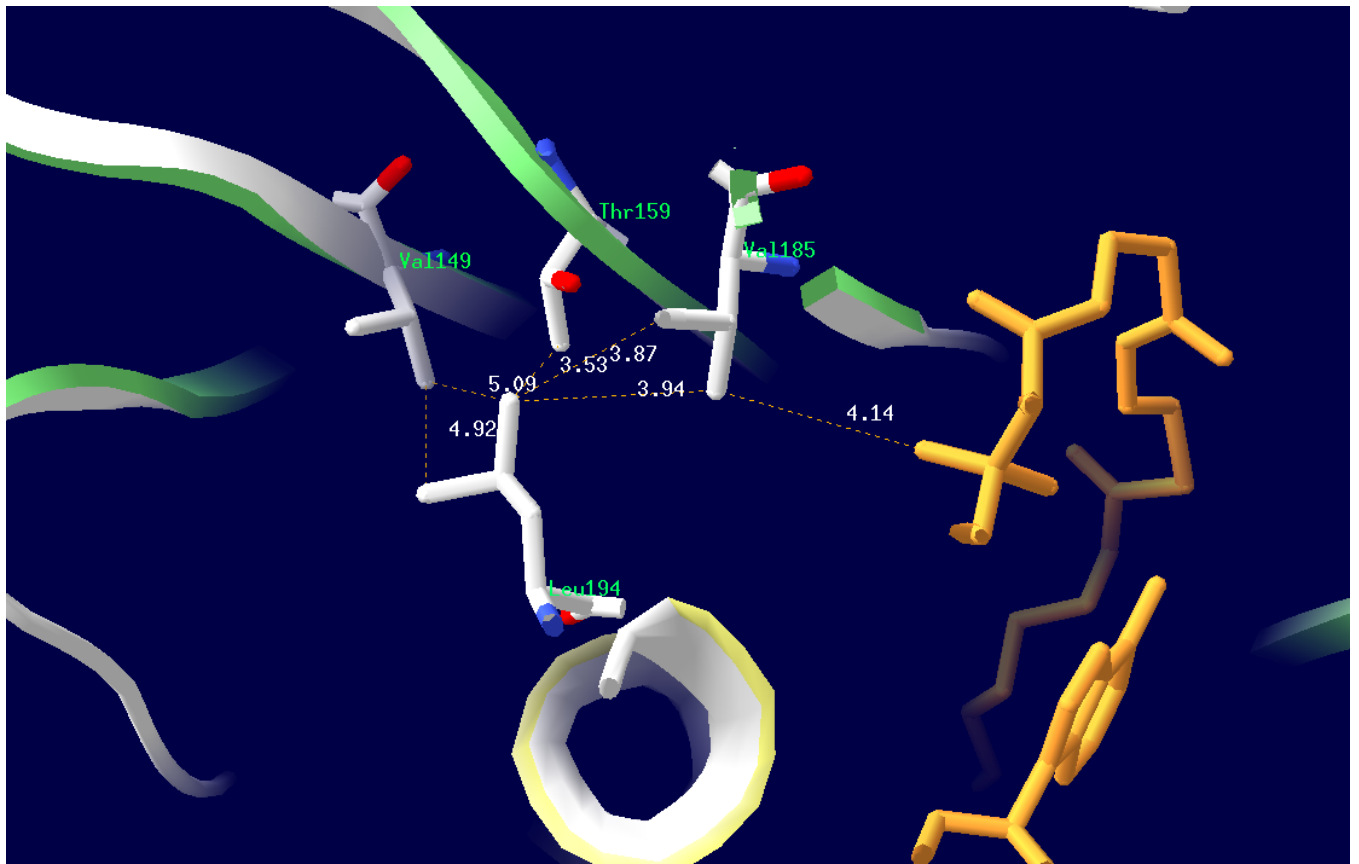
c) Evaluation of salt stress on root elongation, in Col0/SEC-RFP, *STINGY* and *STINGY/NMT1*. The root elongation of *STINGY* was significantly affected by NaCl compared to the other backgrounds. Sample size ≥ 20 seedling each. Error bar are SEM.

Formatted Alignments

	10	20	30
At2g47170	M G L S F G K L F S R L F A K K E M R I L M V G L D A A G K		
At1g10630	M G L S F A K L F S R L F A K K E M R I L M V G L D A A G K		
At3g62290	M G L S F G K L F S K L F A K K E M R I L M V G L D A A G K		
	M G L S F G K L F S R L F A K K E M R I L M V G L D A A G K		
	40	50	60
At2g47170	T T I L Y K L K L G E I V T T I P T I G F N V E T V E Y K N		
At1g10630	T T I L Y K L K L G E I V T T I P T I G F N V E T V E Y K N		
At3g62290	T T I L Y K L K L G E I V T T I P T I G F N V E T V E Y K N		
	T T I L Y K L K L G E I V T T I P T I G F N V E T V E Y K N		
	70	80	90
At2g47170	I S F T V W D V G G Q D K I R P L W R H Y F Q N T Q G L I F		
At1g10630	I S F T V W D V G G Q D K I R P L W R H Y F Q N T Q G L I F		
At3g62290	I S F T V W D V G G Q D K I R P L W R H Y F Q N T Q G L I F		
	I S F T V W D V G G Q D K I R P L W R H Y F Q N T Q G L I F		
	100	110	120
At2g47170	V V D S N D R D R V V E A R D E L H R M L N E D E L R D A V		
At1g10630	V V D S N D R D R V V E A R D E L H R M L N E D E L R D A V		
At3g62290	V V D S N D R D R V V E A R D E L H R M L N E D E L R D A V		
	V V D S N D R D R V V E A R D E L H R M L N E D E L R D A V		
	130	140	150
At2g47170	L L V F A N K Q D L P N A M N A A E I T D K L G L H S L R Q		
At1g10630	L L V F A N K Q D L P N A M N A A E I T D K L G L H S L R Q		
At3g62290	L L V F A N K Q D L P N A M N A A E I T D K L G L H S L R Q		
	L L V F A N K Q D L P N A M N A A E I T D K L G L H S L R Q		
	160	170	180
At2g47170	R H W Y I Q S T C A T S G E G L Y E G L D W L S N N I A S K		
At1g10630	R H W Y I Q S T C A T S G E G L Y E G L D W L S N N I A S K		
At3g62290	R H W Y I Q S T C A T S G E G L Y E G L D W L S N N I A N K		
	R H W Y I Q S T C A T S G E G L Y E G L D W L S N N I A S K		
	190	200	210
At2g47170	A		
At1g10630	A		
At3g62290	A		
	A		

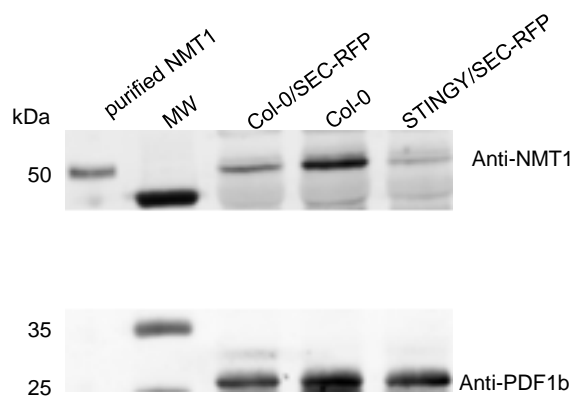
Supplemental Figure 4. Multiple sequence alignment of *A. thaliana* Arf1A1C, ArfA1F and ArfA1E

Alignment of Arf1A1C, ArfA1F and ArfA1E protein sequences run by ClustalW 2.1 multiple sequence alignment shows high similarity at the amino acid level.



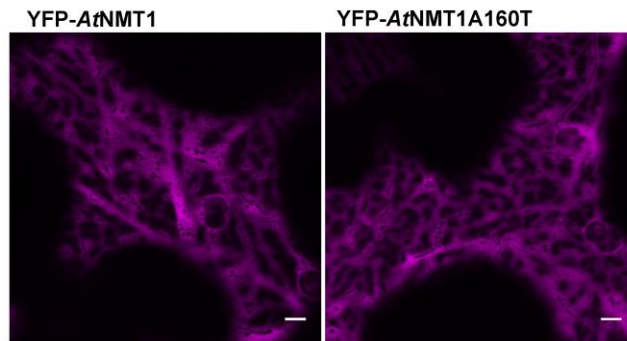
Supplemental Figure 5. Model of NMT1A160T in complex with myristoylCoA.

The 3D model of the A160T variant was aligned with that of the ScNMT-myristoyl-CoA complex. A slab of 10 Å was selected to reveal only the most proximal residues which are displayed. The main secondary structures are shown and myristoyl-CoA is shown in ball and stick in orange. Distances are indicated in Angstroms. In this figure, because Met1 is removed from the mature protein, amino acid 1 corresponds to Ala2 of the open reading frame (ORF). This explains why residue Ala160 of the ORF, which is substituted into Thr in the mutant, is numbered Thr159 in the 3D structure model.



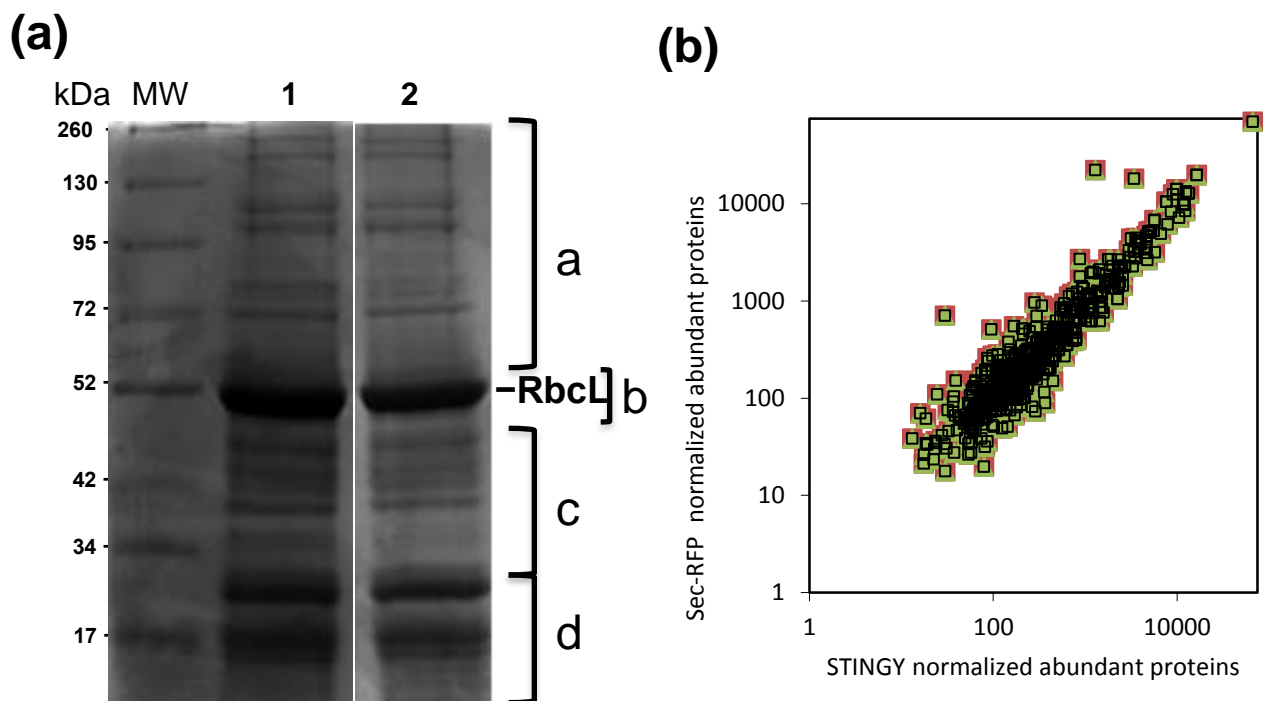
Supplemental Figure 6. *STINGY* shows reduced accumulation of NMT1A160T protein.

Accumulation of NMT1A160T or NMT1 was estimated in each indicated genotype by immunoblot analysis using specific antibodies against NMT1. The equivalent lower membranes were used for normalization by using antibodies against PDF1b. (MW= molecular weight)



Supplemental Figure 7. YFP-NMT1 and YFP-NMT1A160T are distributed in the cytosol.

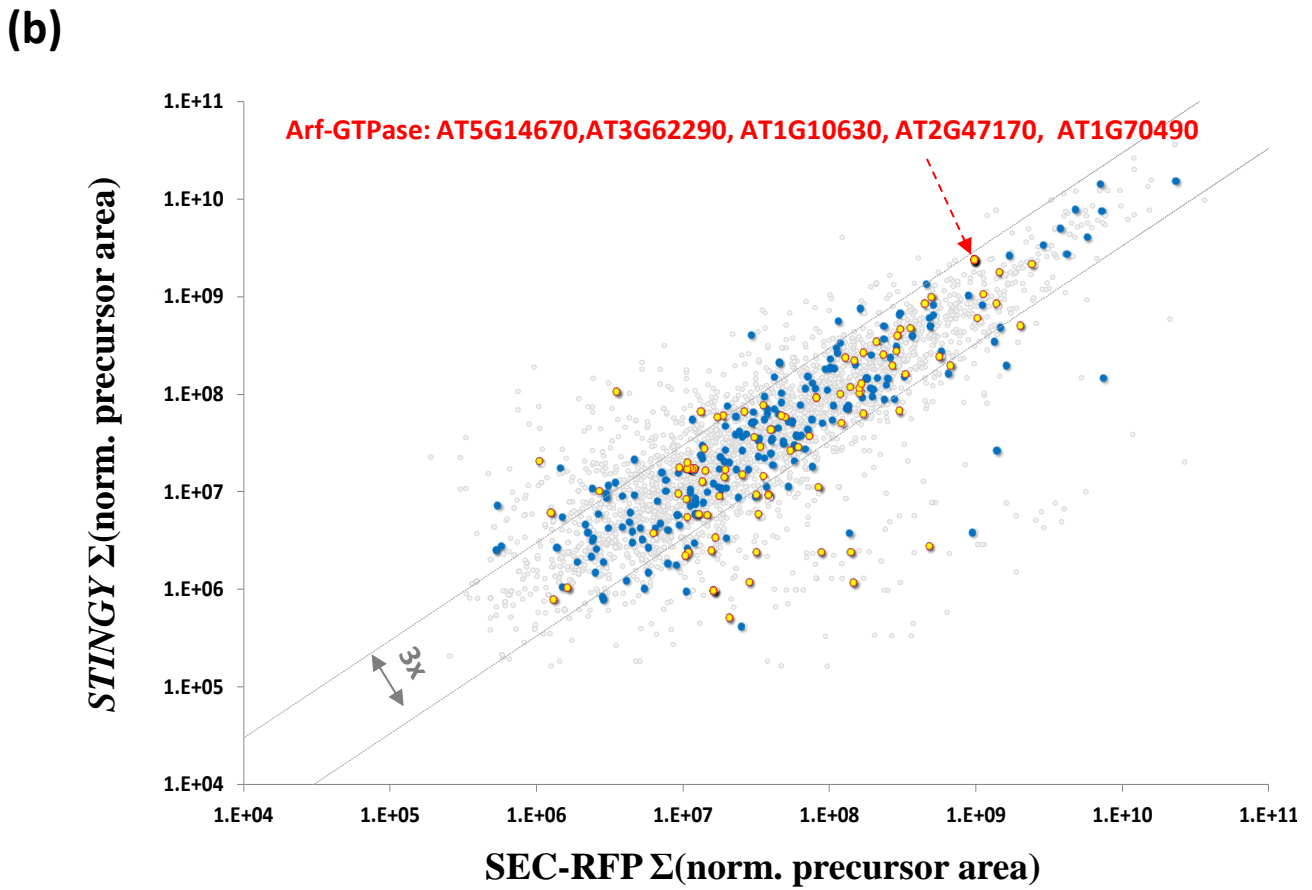
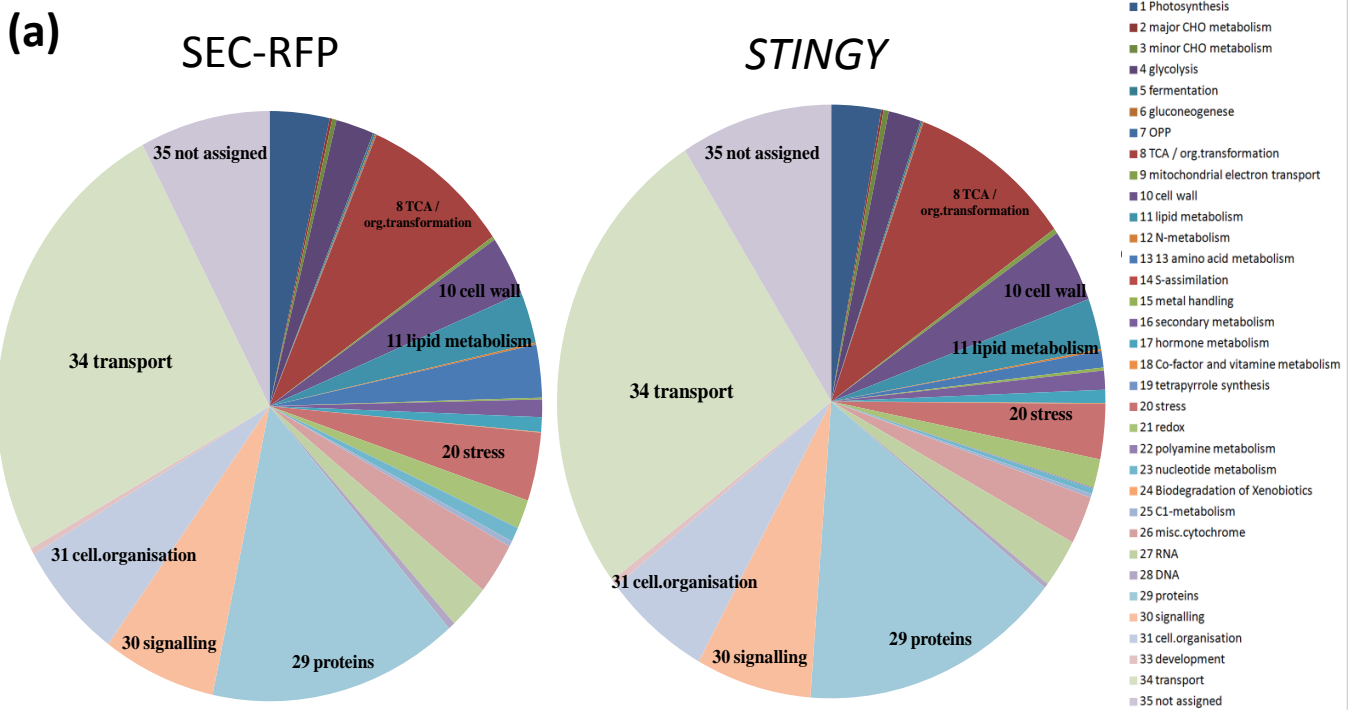
Confocal images of tobacco leaf epidermal cells transiently expressing either YFP fusions of NMT1 or NMT1A160T showing similar distribution in the cytosol. Scale bars = 5 μ m.



Supplemental Figure 8. Proteome analysis of total soluble proteins from leaves of nine-week-old plantlets.

a) 1D-SDS PAGE gel lanes of total soluble proteins (45µg per well) from leaves of *A. thaliana* SEC-RFP (line 1) and *STINGY* (line 2) stained with Coomassie Brilliant Blue. The four bands (a, b, c, d) of each line were analysed by nLC-MS/MS using LTQ-Orbitrap-Velos after in-gel digestion. RbcL, Rubisco large subunit.

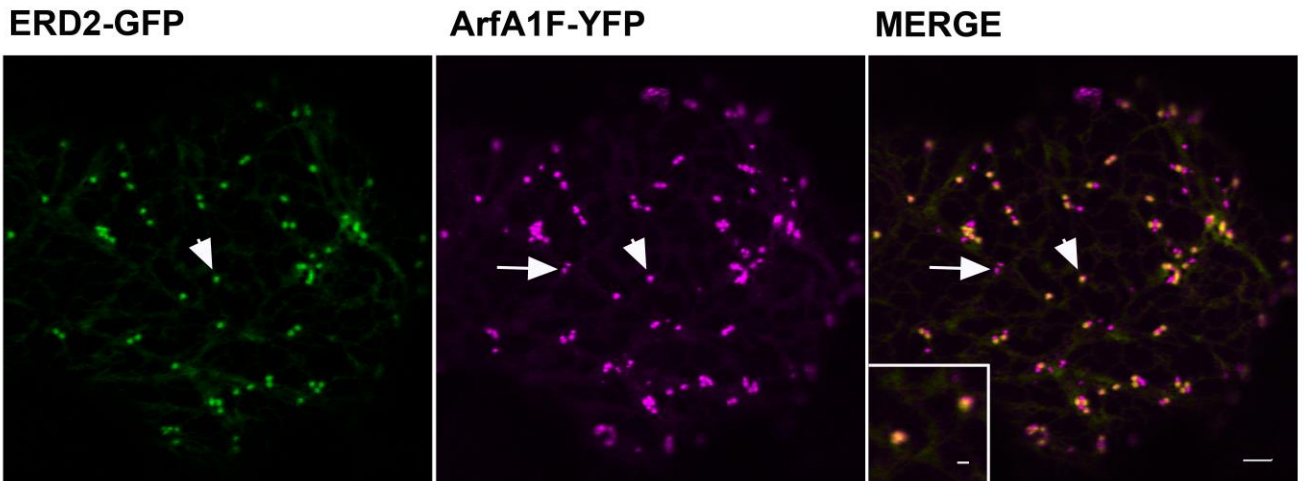
(b) Scatter plot of normalized abundant proteins between Sec-RFP and *STINGY* mutant based on label-free Proteome Discoverer analysis (Thermo).



Supplemental Figure 9. Comparison of SEC-RFP and *STINGY* plasma membrane proteomes.

a) Comparison of protein abundance (based on normalized precursor areas) of the different functional groups (using 35 MapManBin non redundant bins). In both SEC-RFP and *STINGY* plasma membrane enriched fractions more than 60% of mass proteins was distributed in transport (bin 34), protein synthesis and homeostasis (bin 29), signaling (bin 30), cell organization (bin 31) and proteins of unknown or not assigned functions (bin 35). The remaining protein mass was distributed within a varied set of bins. No major changes in protein functional distribution were observed between SEC-RFP and *STINGY*.

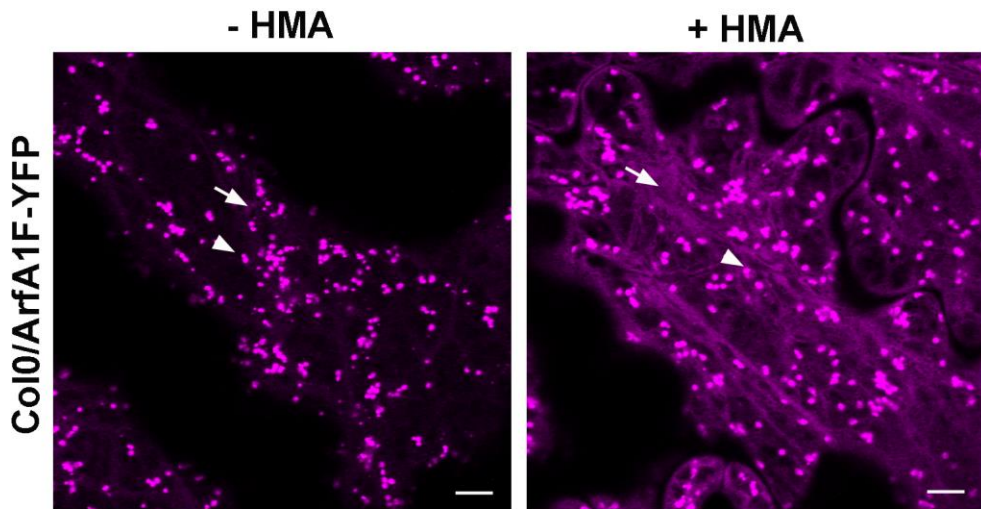
b) Distribution of protein relative abundance (based on normalized precursor areas) between SEC-RFP (x-axis) and *STINGY* (y-axis). Plotted: the total identified proteins (grey), proteins that contain a Gly N-terminal residue (blue), and proteins predicted to be myristoylated (red). Grey lines delineate the region of a <3 fold change in the SEC-RFP/*STINGY* ratio.



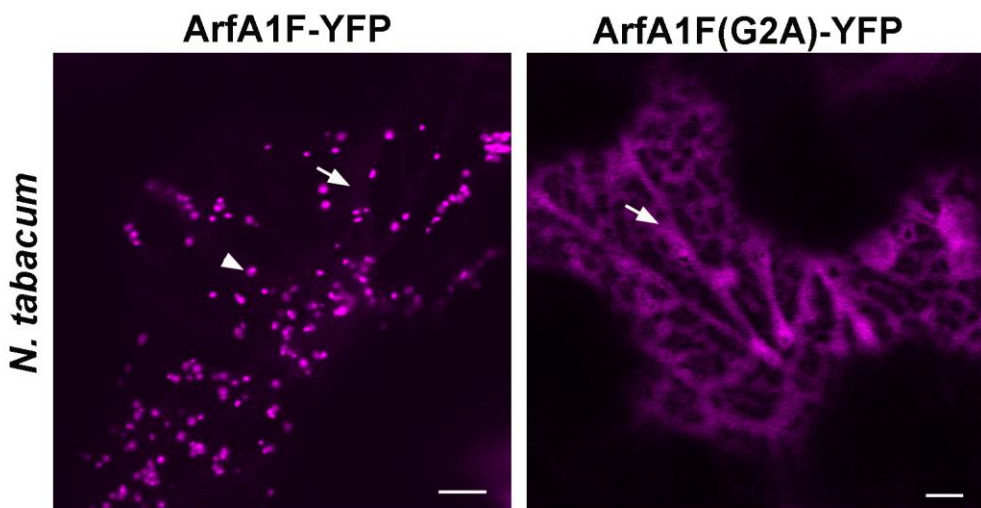
Supplemental Figure 10. ArfA1F-YFP is localized to the Golgi

Confocal images of a tobacco leaf epidermal cell co-expressing ArfA1F-YFP and ERD2-GFP showing co-localization at the Golgi stacks (arrows) and the presence of additional ARFA1F-YFP structures (arrowheads). The inset show a magnification of the colocalization between ArfA1F and ERD2. Scale bar = 5 μm , scale bar in the inset = 1 μm .

a)

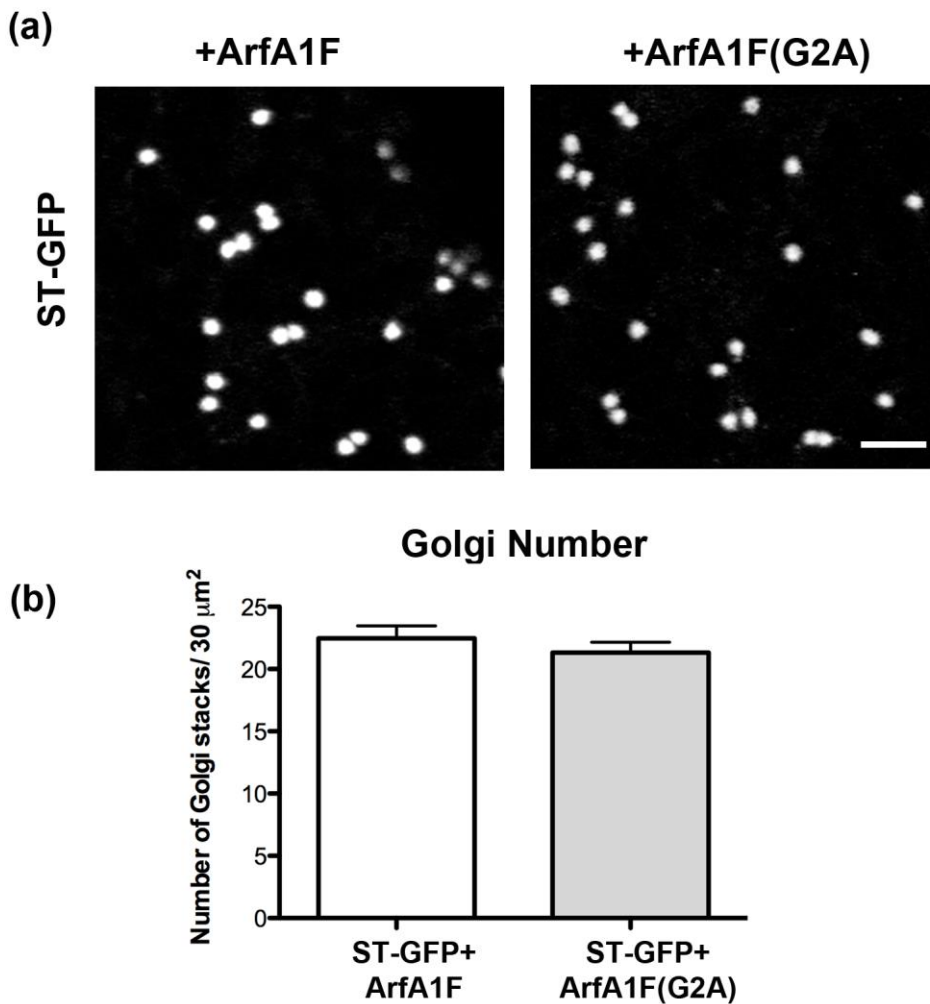


b)



Supplemental Figure 11. HMA treatment and the ArfA1F(G2A) compromise ArfA1F distribution to endomembranes

Confocal microscopy analysis of Arabidopsis leaf epidermal cells treated with HMA showed large redistribution of ArfA1F-YFP in the cytosol (arrows) with respect to the distribution of the protein to punctae (arrowheads). Similarly, analyses of ArfA1F(G2A)-YFP transiently expressed in tobacco leaf epidermal cells showed a cytosolic distribution (arrows) compared to the wild type that is distributed clearly to punctae (arrowheads). Scale bars = 5 μ m.



Supplemental Figure 12. Overexpression of ArfA1F(G2A) does not affect the distribution of the Golgi marker ST-GFP and the Golgi number in cortical regions. Images of tobacco leaf epidermal cells co-expressing ArfA1Fwt, ArfA1F(G2A) and the Golgi marker ST-GFP. Only fluorescence relative to ST-GFP is shown for clarity (panel a). ST-GFP was found in the Golgi both in the presence of wild-type Arf1A1F and Arf1F(G2A). The number of Golgi was also unchanged in such cells as established by the count of Golgi stacks/cortical area regions (panel b). Sample size = 75 areas. Error bars are SEM. Scale bars= 5 μm .

Rank	Locus ID	Paralogs	Score	Linked_query	GO_P	GO_C	GO_F
1	AT2G04350 (LACS8)	no_paralog	4.14	AT5G57020	Fatty acid biosynthetic process	na	Long chain fatty acid CoA ligase activity
2	AT1G54650	no_paralog	3.78	AT5G57020	na	na	na
3	AT3G62290 (ArfA1E)	AT2G47170 (Arf1A1C)	3.45	AT5G57020	na	Intracellular endomembrane system	Protein binding; GTP binding phospholipase activator activity
4	AT2G47170 (Arf1A1C)	AT3G62290 (ArfA1E)	3.32	AT5G57020	na	Golgi-associated vesicle	Protein binding; GTP binding phospholipase activator activity
5	AT1G10630 (ArfA1F)	no_paralog	3.23	AT5G57020	na	na	na
6	AT1G70490 (ArfA1D)	AT1G23490 (Arf1)	3.18	AT5G57020	na	Intracellular mitochondrion	Protein binding; GTP binding phospholipase activator activity

Supplemental Table 1 online. Probabilistic functional gene network of *NMT1*. a) List of top correlated genes with *NMT1*. The score illustrates the probability of interaction, representing a true functional linkage between the two genes. Within the top six genes with the highest score there are ArfA proteins: At3g62290, At2g47170, At1g10630. (na is for not available)

Primer name	Sequence
5` oligonucleotide for NMT1 untagged in PFGC	GTGGCGCGCCATGGCAGATAACAATTCACCACCTGGC
3` oligonucleotide for NMT1 untagged in PFGC	AGGACGTCTAGATTATAAGAGAACAAGCCCGAGTTCCG C
5` oligonucleotide for NMT1 in pEARLY 104	ATGGCAGATAACAATTCACCACCTGGC
3` oligonucleotide for NMT1 in pEARLY 104	TTATAAGAGAACAAGCCCGAGTTCCGC
5` oligonucleotide for ArfA1F in pEARLY_GW 101	ATGGGGCTTTCATTTGCAAAGCTTTTTAGC
3` oligonucleotide for ArfA1F in pEARLY_GW 101	AGCTTTGCTAGCAATGTTGTTGGAAAGC
5` oligonucleotide for ArfA1F (G2A) in pEARLY_GW 101	ATGGCGCTTTCATTTGCAAAGCTTTTTAGC
3` oligonucleotide for ArfA1F (G2A) in pEARLY_GW 101	AGCTTTGCTAGCAATGTTGTTGGAAAGC

Supplemental Table 2 online: Oligonucleotides used for the constructs preparation.